Mon. Not. R. astr. Soc. (1988) **231,** 57–67 and *Microfiche* MN 231/1

Hydrogen absorption line profiles of ionizing star clusters

Angeles I. Díaz* *Royal Greenwich Observatory, Herstmonceux Castle, Hailsham, East Sussex BN27 1RP*

Accepted 1987 September 11. Received 1987 September 11; in original form 1986 July 14

Summary. Model synthesized profiles of the Balmer absorption lines for ionizing star clusters have been constructed for different ages ranging from 1 to 40 Myr and power-law initial mass functions (IMF) of different slopes. These profiles can be used in combination with those corresponding to different stellar populations in order to reproduce the profiles observed in regions of recent star formation and eliminate the effect of contamination of the nebular emission lines by the underlying stellar absorption.

It is found that the computed profiles are rather insensitive to both age and assumed IMF. The widest profiles correspond to an age of 4 Myr and a solar neighbourhood IMF and the narrowest to ages of about 8–9 Myr and a value of the IMF slope of about 1.35.

1 Introduction

A classical problem hampering the spectral analysis of composite systems in which star formation is seen to be efficient at the current epoch, has been the contamination of the nebular Balmer emission lines by an absorption component of stellar origin. This contamination is probably negligible in the case of Hα but becomes increasingly important for higher terms of the Balmer series. Obviously, accurate measurements of the nebular hydrogen emission line strengths are essential to deduce important information concerning these systems, e.g. present rate of star formation, excitation parameter ([O III] λ5007/Hβ), chemical abundances and internal interstellar reddening.

Population synthesis provides a means for correcting observed nebular hydrogen emission line strengths for underlying stellar absorption. The usual approach is to fit stellar population models to agree with the observed equivalent widths of relevant absorption lines (e.g. Alloin & Kunth 1979) or continuum colours and spectral energy distributions (e.g. Hunter, Gallagher & Rautenkranz 1982) and use the deduced strengths of the Balmer absorption lines to eliminate their contribution to emission. In general, these are linear programming techniques that combine

*Present address: Universidad Autónoma de Madrid, Departamento de Física Teórica C-XI, Ciudad Universitaria de Cantoblanco, 28049 Madrid, Spain.

contributions to the total integrated spectrum by different stellar groups and try to find an optimal solution by minimizing the residuals between models and observations. Two problems arise with these kinds of models. First, the solution obtained is usually not unique and second, a very complete stellar library is needed. The solution of the second problem, i.e. the introduction of more stellar groups with different metallicities and luminosity classes, leads to a worsening of the first through the introduction of more free parameters. Some astrophysical constraints, like fixing the relative number of evolved and unevolved stars, are usually imposed in order to restrict the number of possible solutions. In some cases, no constraints at all are employed (Hunter *et al.* 1982).

In what follows, a different approach to the problem is presented, based on the study of the absorption line profiles of the Balmer lines. In fact, the hydrogen line profiles associated with an old stellar population, either metal poor (e.g. a metal poor globular cluster) or metal rich (e.g. an elliptical galaxy) are very different from the broad profiles often observed in composite systems where star formation is important; these latter ones resemble more the profiles characteristic of early A stars near the main sequence (see, e.g. Díaz *et al.* 1982 and Díaz 1985). It is therefore of interest to calculate the contribution to the profiles observed in these regions by the young stellar component which characterizes the starburst.

If the region we observe is assumed to be ionized by a young stellar cluster, its age cannot exceed a certain limit. This limit depends on several parameters, mainly the ones characterizing the initial mass function (IMF), i.e. the mass spectrum with which stars are born, and the metal content of the region; it never exceeds 10 Myr (Dottori 1981; Melnick, Terlevich & Eggleton 1985). The equivalent width of the Hβ emission line can be calculated for different starburst models at a given age (e.g. Dottori 1981) and a maximum contribution by such a burst to the total observed stellar continuum can be calculated from the ratio of the calculated and measured Hβ emission equivalent widths.

We have constructed synthetic hydrogen absorption line profiles for starbursts of solar metallicity and several discrete ages ranging from 1 to 40 Myr. These can be used in combination with the profiles corresponding to different stellar populations of varying ages and metallicities in order to reproduce the ones observed in star forming regions.

Section 2 of this work offers a description of the models. The results are presented in Section 3 and Section 4 presents the example of an application to a real case: the nucleus of NGC 7552. Finally, the conclusions of this work are given in Section 5.

2 Description of the models

The models are computed by evolving star clusters formed with a given IMF along their corresponding theoretical evolutionary tracks to different ages. Recent studies of the evolution of giant H II regions (Terlevich 1982, 1985) suggest that the IMF can be well represented by a single power-law mass spectrum in the mass range $0.1 \leqslant m \leqslant 100\, M_\odot$, whose slope is a strong function of the metallicity. Therefore, although our star clusters are all of solar metallicity, we have computed models with a single power-law IMF [$\phi(m) \propto m^{-(1+x)}$] of different slopes: $x = 1.35, 2.05, 2.35$ and 2.65 corresponding to 0.2, 1, 2 and 4 times the solar metallicity. It is implicitly assumed that in this range of metallicity the stellar evolution will not be very different from the solar case. We have also computed models with an IMF equal to that observed in the solar neighbourhood (SN) (Miller & Scalo 1979) as parametrized by Tinsley (1980).

In the range of ages we are interested, i.e. 1–10 Myr, only the most massive stars ($m > 20\, M_\odot$) evolve off the main sequence. Evolutionary tracks for these massive stars have been taken from Chiosi, Nasi & Sreenivasan (1978). The rest of the stars in the cluster remain on the zero age main sequence (ZAMS) which has been taken from Bruzual (1982).

Our procedure assumes the starburst to be instantaneous or that its duration is much shorter than the lifetimes of the stars involved. This is certainly not true since real clusters will take a finite time to form, probably of the order of 10 Myr (see Melnick 1985 and Melnick *et al.* 1985), comparable with the ages of the stars we are considering. Therefore, any real star cluster will be a combination of the ones we have modelled. However, as we will see in Section 4, the hydrogen absorption line profiles and equivalent widths are not very sensitive to small variations in age for $t \leqslant 4\times10^7$ yr, so that our procedure seems to be justified.

At a given burst age (time) the effective temperature and luminosity of stars of a given initial mass were read from their corresponding evolutionary tracks. Every evolutionary stage characterized by the pair of values $T_{\rm eff}$ and L, we will denote by j.

Following de Vaucouleurs & de Vaucouleurs (1958) we define $k_{j,\lambda}$, the contribution of stars in stage j at wavelength λ, to be

$$k_{j,\lambda}=N_j\cdot f_{j,\lambda}\Big/\sum_j N_j\cdot f_{j,\lambda}$$

where N_j is the number of stars in evolutionary stage j and $f_{j,\lambda}$ is the corresponding flux at wavelength λ. The equivalent width of a line at wavelength λ is then:

$$W_\lambda=\sum_j k_{j,\lambda}\cdot W_{j,\lambda}$$

where $W_{j,\lambda}$ is the equivalent width of that line in a star in evolutionary stage j. In the same way, if we denote the profile of a given hydrogen line by $P(\mathrm{H}\lambda)$, we can write

$$P(\mathrm{H}\lambda)=\sum_j k_{j,\lambda}\cdot P_j(\mathrm{H}\lambda)$$

where $P_j(\mathrm{H}\lambda)$ is the corresponding hydrogen line profile of a star in stage j.

Profiles of the Balmer absorption lines Hδ, Hγ, Hβ and Hα have been calculated by Kurucz (1979) for an extensive grid of model stellar atmospheres with effective temperatures in the range $5500 \leqslant T_{\rm eff} \leqslant 50\,000$ K, surface gravities in the range $0.00 \leqslant \log g \leqslant 5.00$ and metallicities 1, 0.1 and 0.01 $Z_\odot$. They are presented as residual fluxes normalized to a continuum of 1000 units at ± 100 Å from the line centre. For stars of $T_{\rm eff} < 5500$ K we have taken the profiles given by Vidal, Cooper & Smith (1973) normalizing them in the same way.

For the sake of consistency, we have taken the spectral energy distributions (SED) given by Kurucz's (1979) models for stellar types for whose effective temperatures and surface gravities are in the range used for those computations. For the rest of the stars we have adopted the empirical SEDs given by Straizys & Sviderskiene (1974). They have been converted to absolute fluxes by using the transformations from theoretical to observational parameters given by Flower (1977) and the absolute visual magnitudes, M_V, given by Allen (1973) for each stellar type.

3 Model results

The model results are presented in Tables 1–5 (see *Microfiche* MN 231/1) for different initial mass functions, one corresponding to the SN and four single power laws of different slope, and ages 0, 4, 6, 8, 20 and 40 Myr. The tables give the profiles of the Balmer absorption lines Hδ, Hγ, Hβ and Hα as residual fluxes from the continuum, normalized to 1000 units at ± 100 Å from the centre of the line. Also given in the tables are the equivalent widths of the lines.

Fig. 1 shows an example of the model results. In this case it corresponds to the model of 4 Myr computed with a solar neighbourhood IMF. The hydrogen absorption line profiles have a very similar appearance for all the computed star clusters. The differences among them are illustrated

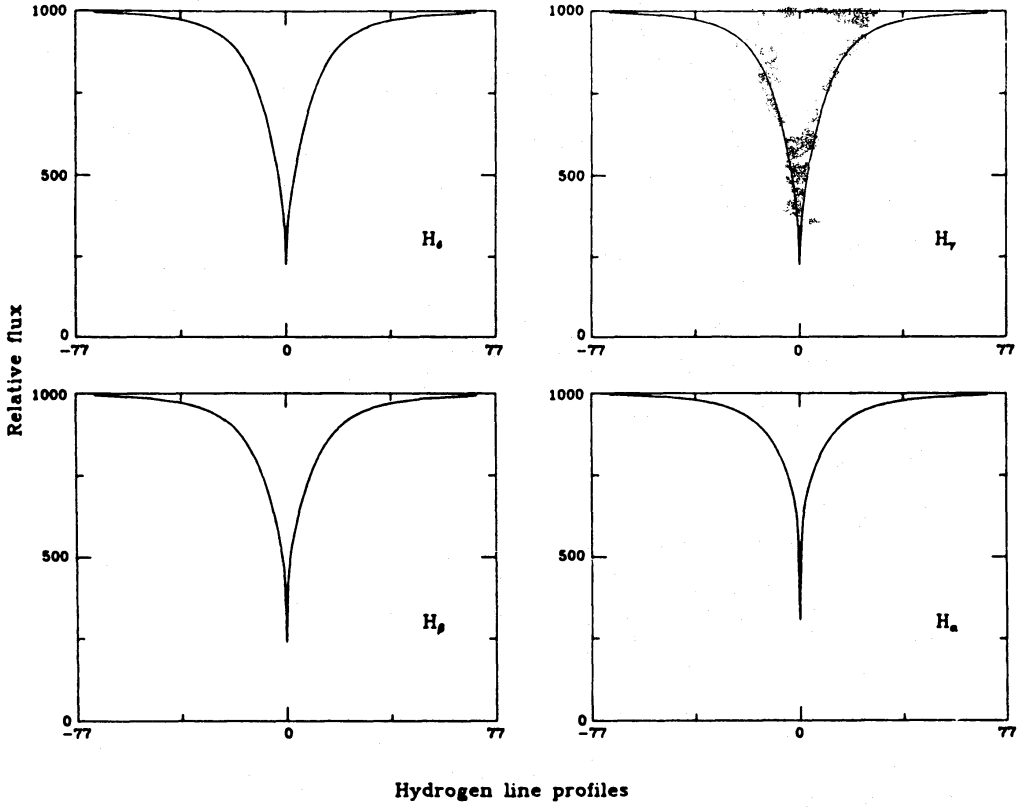

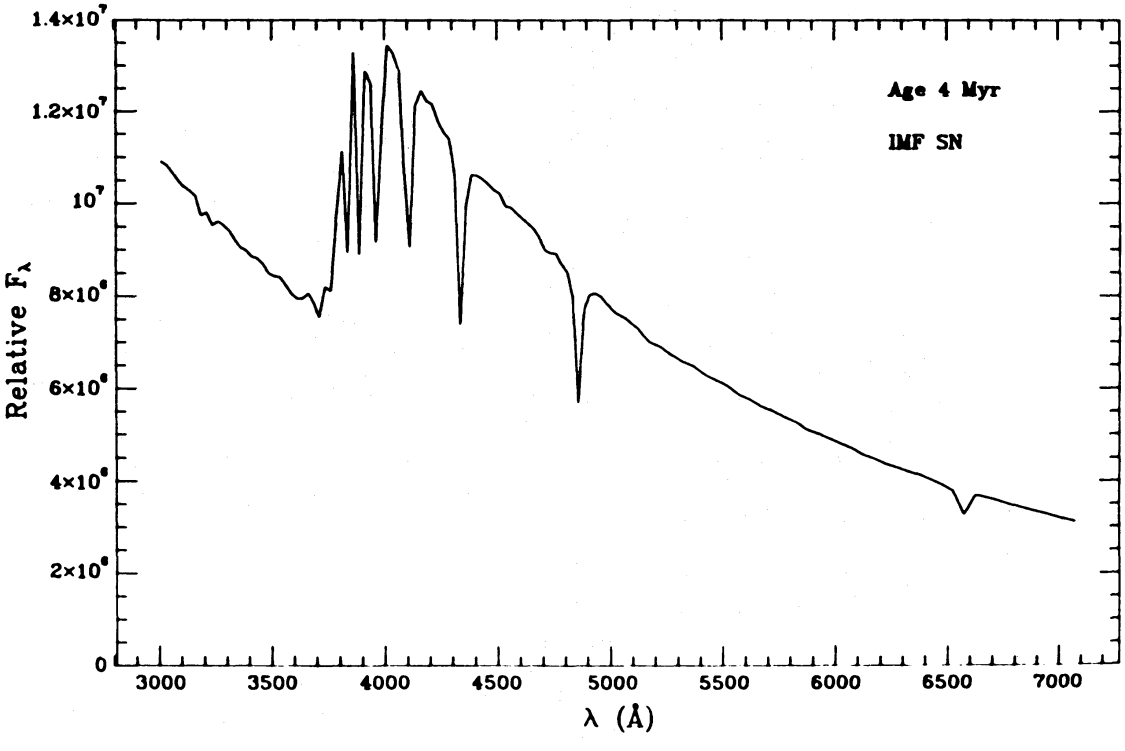

Figure 1. Model computed hydrogen line profiles and spectral energy distribution for a star cluster 4 Myr old formed with a solar neighbourhood initial mass function.

in Figs 2 and 3. Fig. 2 shows the profiles of the Hδ absorption line corresponding to ionizing clusters of different ages formed with a SN IMF. The profile widens as the cluster evolves from 0 to 4 Myr and it becomes slightly narrower again for ages between 6 and 8 Myr. At an age of 10^9 yr, included here for comparison purposes, the lines become appreciably narrower as the A stars, mainly responsible for the broad hydrogen absorption lines, begin to evolve off the main sequence.

Changes in the IMF can also affect the profile shapes of the lines as the contribution of different stellar groups to the total continuum changes. Fig. 3 shows the variation in the Hδ absorption line profiles for star clusters 4 Myr old computed using different assumptions about the IMF. The largest contribution from dwarfs is found for the SN IMF while the smallest one corresponds to

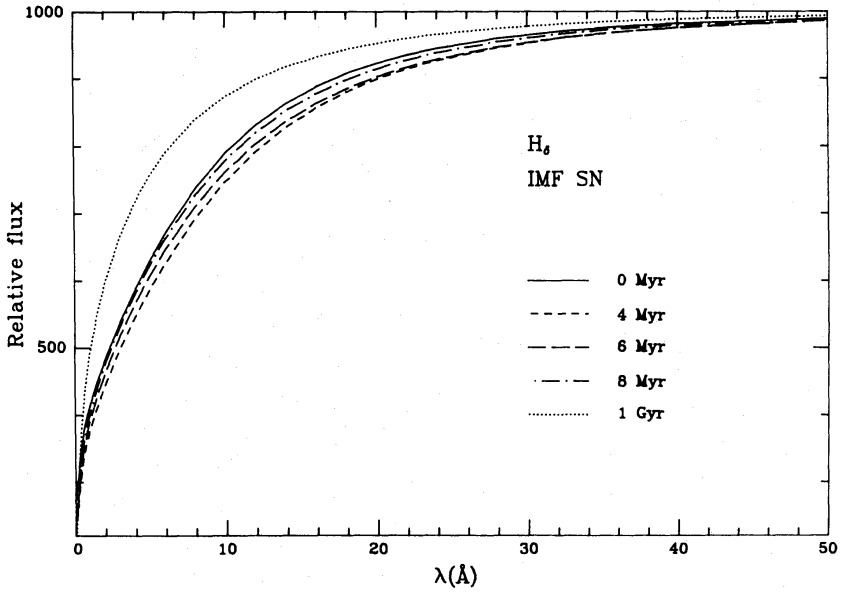

Figure 2. Hydrogen Hδ absorption line profiles for starbursts of different ages, computed with a solar neighbourhood initial mass function.

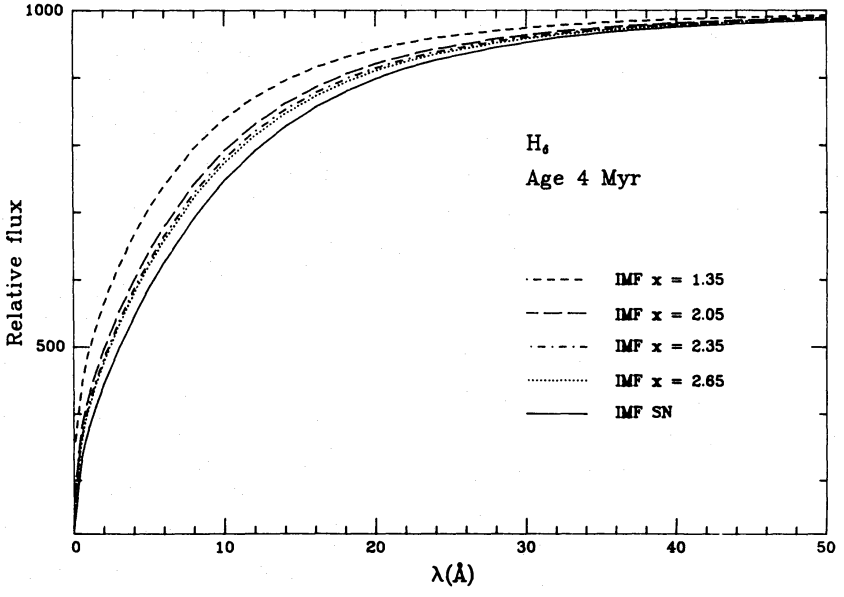

Figure 3. Same as Fig. 2 but for starbursts 4 Myr old computed with different initial mass functions as indicated in the figure.

the flatter Salpeter's one ($x=1.35$). If Terlevich's (1982) relationship is used, this latter IMF slope would correspond to a metallicity of $0.2\,Z_{\odot}$.

Our models therefore show that, for the range of ages suitable for a young ionizing star cluster, the hydrogen absorption line profiles are rather insensitive to both the age of the burst and the assumed IMF. The largest contribution from dwarfs, and therefore the widest profiles, is found for an age of about 4 Myr and a SN IMF. At the other extreme, the smallest contribution from dwarfs would correspond to an age of about 8–9 Myr (close to the limiting age for hydrogen ionization) and an IMF of constant slope, corresponding to a low metallicity of the order of $0.2\,Z_{\odot}$.

The model equivalent widths of the hydrogen absorption lines range from 9 to 15 Å for Hδ, corresponding to zero-age cluster computed with a single power-law IMF of $x=1.35$ and a starburst 4 Myr old computed with a SN IMF. Similar ranges in equivalent widths are found for the Hγ and Hβ lines: for Hα the range is somewhat narrower [$7 \leqslant \mathrm{EW(H}\alpha) \leqslant 10$ Å]. These equivalent widths are computed by integrating along the line profile over ± 100 Å from the line centre. This has to be taken into account when using these equivalent widths for the correction of nebular lines whose full widths at zero intensities (FWOI) are much smaller. The contribution of the core of the line (± 5 Å from the centre) to the total equivalent width is about 40 per cent, but depending on the spectral resolution the fraction of the line actually filled in by emission can be much smalier.

The comparison of the model results with the observations is very difficult due to the lack of the necessary good quality data. Values for the contribution of the Hδ, Hγ, Hβ and Hα absorption to the emission equivalent widths in blue compact galaxies, giant extragalactic H II regions and H II galaxies are estimated to be between 1 and 2 Å only (Kunth & Sargent 1983; McCall, Ribsky & Shields 1985; Campbell 1986), about two to four times smaller than the calculated equivalent widths for the very core of the lines. No absorption wings are detected in most cases but this could be due to the poor signal-to-noise in the continuum. It is also possible that the small aperture used in these observations does not include the whole of the star cluster but rather the most massive stars only. For some of the H II galaxies observed by Campbell (1986), data obtained with larger apertures seem to show wide wings in the hydrogen absorption lines (R. Terlevich, private communication). Some authors have suggested that the IMF might be truncated at somewhere between 3 and $20\,M_{\odot}$ (e.g. Rieke *et al.* 1980; Viallefond & Thuan 1983; Augarde & Lequeux 1985). In this case, we do not expect to observe Balmer absorption lines. They are observed, however, in the super star cluster NGC 1705 (Melnick, Moles & Terlevich 1985) although they are seen to be weaker than predicted by the models. The measured equivalent width of Hδ, the least affected by emission, is 4.0 Å (J. Melnick, private communication) compared with the predicted value of 13 Å for a cluster age of 10^7 yr and an IMF of slope $x=2.05$. Of course, the possibility cannot be excluded of the existence of an underlying stellar population which might provide a substantial contribution to the continuum. Higher resolution would be needed in order to examine the line profile in detail.

4 Application to an H II-region galactic nucleus

The model computed profiles presented in the previous section can be used to correct the nebular emission lines for the stellar contribution. An application of this procedure has been made for the nucleus of the early barred spiral NGC 7552 whose spectrum shows characteristics of an H II region of low excitation and high abundance (see Ward *et al.* 1980 and Díaz 1985). In this case, the presence of the Balmer absorption lines complicates the measurements of the emission lines, significantly affecting the reddening determination.

The observed emission equivalent width in this galaxy with no correction at all is 5.9 Å. According to the models by Dottori (1981) for solar composition and an IMF of slope $x=1.45$, the

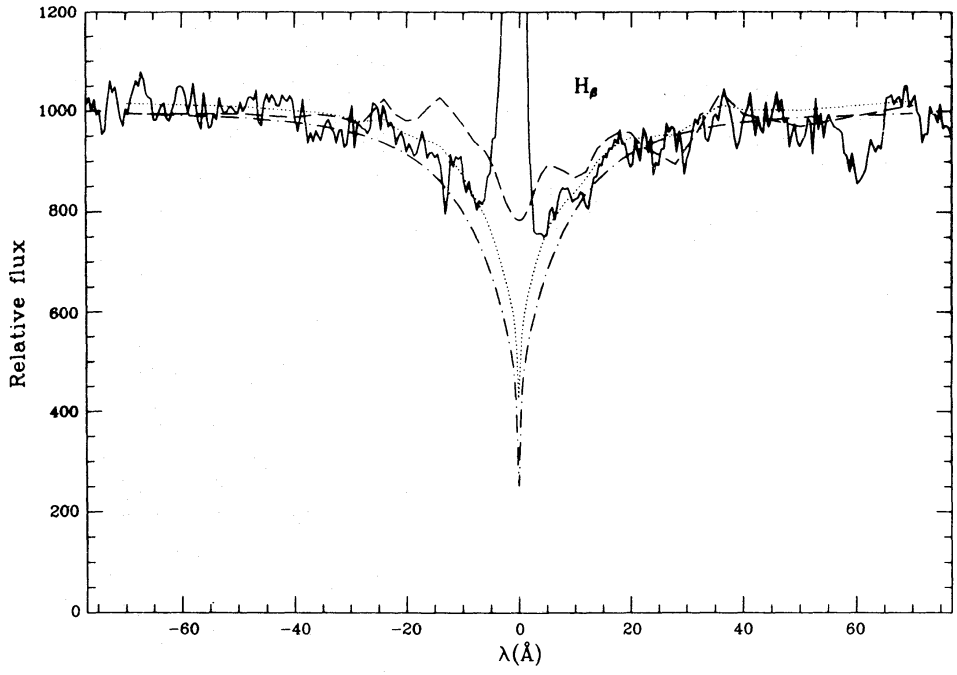

Figure 4. Observed (solid line) and model computed absorption profiles of Hβ for NGC 7552. The resolution of the data is 1.5 Å and the profiles are normalized to 1000 units at the continuum at ±100 Å from the line centre. Details of the models are given in the text.

theoretical emission equivalent widths for ionizing clusters with ages between 1 and 9 Myr are between 573 and 7 Å respectively. Therefore, in order to reproduce the observed Hβ emission equivalent width, the contribution of the ionizing star cluster must lie between 1 per cent in the case of the younger cluster and 80 per cent in the case of the oldest one. However, if we assume the population of the nucleus of NGC 7552 to be similar to that of an elliptical galaxy, which seems to be a reasonable assumption given the early morphological type of this galaxy (Sab), only a few combinations of cluster and underlying galaxy can adequately fit the observed Balmer absorption line profiles.

Fig. 4 shows the absorption profile of Hβ for NGC 7552 observed with a resolution of 1.5 Å (continuous line) normalized to 1000 units at the continuum at ±100 Å from the centre of the line. Also plotted in this figure are the profiles corresponding to two extreme models which reproduce the observed Hβ emission equivalent width: the broken line corresponds to a young cluster (4 Myr) contributing 10 per cent of the total light at Hβ and the old underlying population contributing the remaining 90 per cent; the dash-dotted line corresponds to an old cluster (9 Myr) and the old population contributing 80 and 20 per cent respectively to the total light at Hβ. Widening effects due to velocity dispersions in various stellar groups have not been considered. These can also widen the absorption lines in galactic nuclei and therefore one might think that their profiles depend somehow on the galaxy type through the shape of the gravitational potential in the central regions, and on the instrumental profile. However, the main effects of the velocity dispersions and spectral resolution are to be found in the core of the lines and not in the wings which is the only criterion involved in the fitting. The equivalent widths of the lines are conserved. Bearing in mind that the Balmer absorption profiles are rather independent of age and IMF, it can be seen from the figure that only combinations of cluster and old population in which the cluster contribution to the total flux at Hβ lies between 50 and 70 per cent are possible. This restricts the age of the cluster to 7–9 Myr. The dotted line in the figure corresponds to the model that best fits the observed profiles: the combination of a star cluster 8–9 Myr old computed with a SN IFM

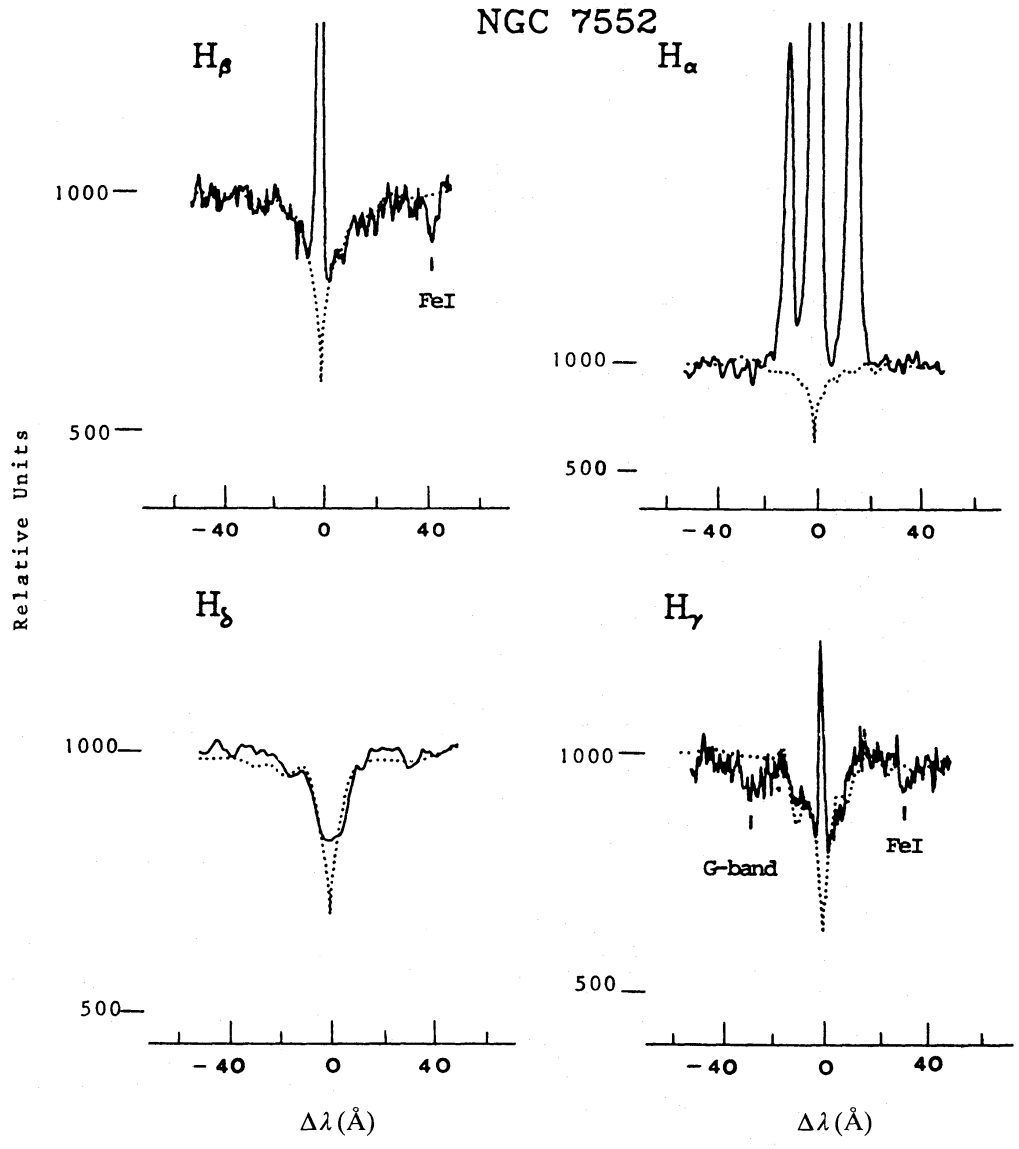

Figure 5. Observed (solid line) and model computed (dotted line) profiles of the hydrogen absorption lines in NGC 7552. Details of the model are given in the text.

contributing 60 per cent of the total flux at Hβ and the old stellar component contributing the remaining 40 per cent.

Fig. 5 shows the fit to the Balmer absorption line profiles. The continuum SED corresponding to the model is shown in Fig. 6 superimposed on the low resolution spectrum of NGC 7552. The resolution of the model has been adjusted to the spectral resolution of the data. The apparent difference in the widths of the lines in the higher terms of the Balmer series is due mostly to an imperfect match of the continuum level in the blue part of the spectrum, which is not surprising given the strong simplifications of the model. The 10 per cent difference between model and observation at the red end of the spectrum may be attributed to 10 per cent errors in the flux calibration (see Díaz 1985).

As a further check on this procedure, we have computed the equivalent widths of the most prominent absorption lines in our model from the corresponding equivalent widths of stars of different spectral types and luminosity classes (D. Alloin, private communication). The comparison of these equivalent widths with the measured ones is shown in Table 6. The general

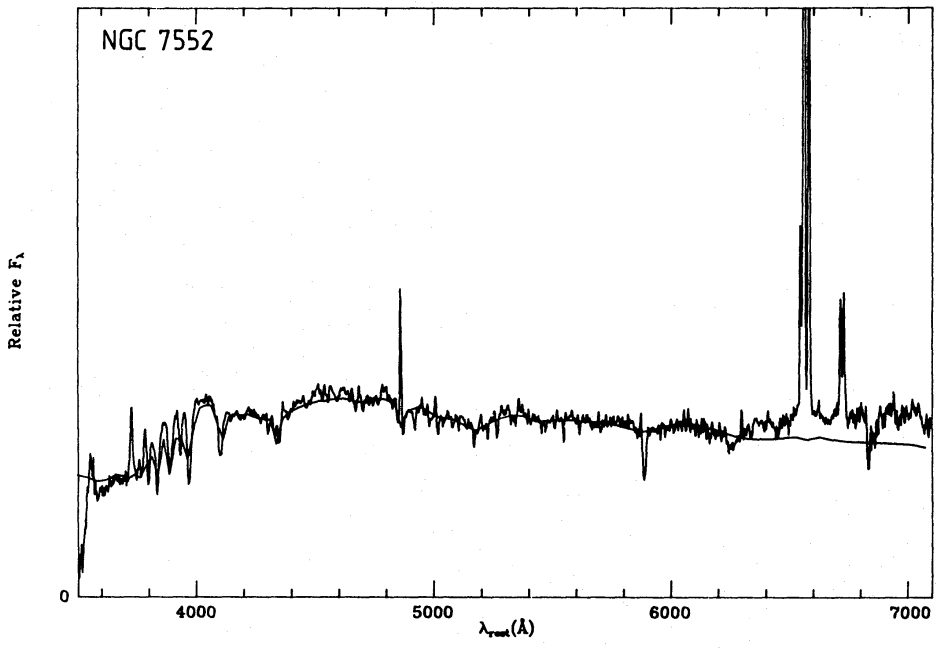

Figure 6. Observed and model computed spectral energy distributions in NGC 7552. Details of the models are given in the text.

Table 6. Observed and computed equivalent widths (Å) in NGC 7552.

Line	λ(Å)	NGC 7552	Model
Ca II *K*	3933	3.17	8.94
Ca II *H*+Hε	3967	8.09	10.09
Hδ	4102	7.17	7.54
Ca I	4226	0.65	1.07
G band	4300	2.00	3.89
Hγ	4340	–	7.72
Hβ	4861	–	8.16
Mg I	5184	2.04	2.49
Na I	5890	5.15	3.19
Hα	6563	–	5.44

agreement is seen to be good. Most of the metal lines are weaker in the galaxy than in the model although the difference is not very large, except in the case of the Ca II *K* line. Differences in the computed and measured equivalent widths of this line can easily arise from different placements of the continuum in the galaxy and in the stars which form the basis of the synthesis. The discrepancies found for the rest of the lines are probably due to differences in metallicity between the elliptical galaxy typifying the old stellar component and NGC 7552. The strong Na I λ5890 Å line observed could not be interstellar in origin.

The subtraction of the profiles we have determined from the observed ones allows the accurate determination of the 'true' values of the Balmer emission line intensities. Table 7 gives these intensities as measured without any correction for underlying stellar absorption and corrected using our profile-fitting technique. With a resolution of 1.5 Å, the corrected value of Hγ turns out to be 1.59 times that observed, while in the case of Hβ the corrected value is only 1.12 times the observed one. Therefore the corrected Balmer decrement Hγ/Hβ is 1.40 times that observed. For Hα the underlying absorption is only 1 per cent of the emission but the observed Hα/Hβ ratio

Table 7. Observed and model-corrected Balmer emission lines in NGC 7552.

Line	Observed			Absorption corrected			Reddening corrected	
	F_λ^*	F_λ/F_β	EW(Å)	F_λ^*	F_λ/F_β	EW(Å)	I_λ^*	I_λ/I_β
Hδ	–	–	–	0.30	8:	0.49	18.4	15
Hγ	0.73	22b	1.27	1.16	30b	2.02	60.0	48
Hβ	3.39	100a	5.88	3.80	100a	6.60	123.0	100
Hα	36.21	1068a	62.80	36.57	961a	63.43	362.9	295

*Units of 10^{-14} erg cm^{-2} s^{-1} arcsec^{-2}. Errors: $a \leqslant 5$ per cent, 5 per cent$\leqslant b \leqslant$10 per cent: factor of 2 uncertainty.

is affected by the correction in Hβ and its corrected value is only 0.90 times the observed one. No high resolution data exist for the Hδ spectral region. This line is not observed in emission and the value given in the table results from the subtraction of the model-computed absorption line from that observed in the low resolution (~6 Å) spectrum. These facts make this value very uncertain.

The reddening constant at Hβ, $c(H\beta)$, is 1.51±0.06 if determined from the Hα/Hβ decrement and 1.44±0.31 when the Hγ/Hβ decrement is used. The agreement is very good and well within the quoted errors which refer to photon statistics and continuum placement. This reddening correction gives a value of Hδ/Hβ=0.15, smaller than the theoretical one by a factor of 1.7 but still within the factor of 2 uncertainty assumed for our value of Hδ.

Our values of the reddening constant, 1.51, and the equivalent width of Hβ in emission, 6.6 Å, are to be compared with those of 0.65 and 11.1 Å estimated by Ward *et al.* (1980). They measure an Hβ emission equivalent width of 7.2 Å while we measure only 5.88 Å. However, the main reason for the large final discrepancy is to be found in the different correction method employed. Ward *et al.* follow the widely extended procedure of predicting the Hβ absorption equivalent width from a given stellar population model and just adding that value to their measured emission equivalent width. They chose model I of Alloin & Kunth (1979) which gives $W_{abs}(H\beta)$=3.9 Å. Therefore they obtain a 'corrected' value of $W_{em}(H\beta)$=11.1 Å. This procedure leads to an overestimation of $W_{em}(H\beta)$ since, as can be seen from their fig. 1 (see also Figs 4 and 5 in this work), the emission does not fill in the whole absorption line but only about 25 per cent of it. Our method allows us to determine which fraction of the absorption line is actually filled in by emission, at a given spectral resolution, and therefore leads to a more accurate correction of $W_{em}(H\beta)$.

5 Conclusions

We have computed synthetic profiles of the Balmer absorption lines for ionizing star clusters based on theoretically predicted stellar profiles, by evolving star clusters of solar metallicity, formed with a given IMF, along theoretical evolutionary tracks to a given age. The range of ages for which we have computed models span from 0 to 40 Myr, 10 Myr being the limiting age for hydrogen ionization by a young star cluster. Different slopes for the IMF, taken to have a power-law form, have been considered. These may be taken to correspond to different values of the cluster metallicity if the slope of the IMF is assumed to depend on it. Models have also been computed with a solar neighbourhood IMF.

The computed profiles are shown to be rather insensitive to variations in age and slopes of the IMF. The widest profiles, implying the largest contribution from dwarfs, are found for clusters 4 Myr old and a SN IMF. Conversely, the sharpest profiles correspond to ages of 8–9 Myr and a flatter (x=1.35) IMF.

These model computed profiles have been used in combination with those observed in an

elliptical galaxy, taken as the prototype of an old stellar population, to reproduce the profiles observed in the nucleus of the SBab galaxy NGC 7552. It is found that a combination of a young star cluster 8–9 Myr old and an old stellar population in proportions 0.6 and 0.4 respectively can adequately fit the observed profiles. This combination also reproduces the observed SED and the equivalent widths of the most prominent absorption lines in this galaxy.

The subtraction of these profiles from the ones actually observed allows the emission line fluxes and equivalent widths to be corrected for absorption by the underlying stellar population and therefore a more accurate determination of the reddening and the hydrogen emission line strengths and equivalent widths.

Acknowledgments

I thank Danielle Alloin and Bernard Pagel for very useful comments and suggestions, and the hospitality of the Observatory of Paris at Meudon where the first version of this paper was written.

Financial support from the American Astronomical Society through the grant of the Henri-Chretien Award and the French Ministry of National Education is kindly acknowledged.

References

Allen, C. W., 1973. *Astrophysical Quantities,* 3rd edn, Athlone Press, University of London.
Alloin, D. & Kunth, D., 1979. *Astr. Astrophys.,* **101,** 372.
Augarde, R. & Lequeux, J., 1985. *Astr. Astrophys.,* **147,** 273.
Bruzual, G., 1982. *PhD thesis,* University of California, Berkeley.
Campbell, A. W., 1986. *PhD thesis,* University of Cambridge.
Chiosi, C., Nasi, E. & Sreenivasan, S. F., 1978. *Astr. Astrophys.,* **63,** 103.
de Vaucouleurs, G. & de Vaucouleurs, A., 1958. *Lowell Obs. Bull.,* **92,** 58.
Díaz, A. I., 1985. *DPhil thesis,* University of Sussex.
Díaz, A. I., Pagel, B. E. J., Edmunds, M. G. & Phillips, M. M., 1982. *Mon. Not. R. astr. Soc.,* **201,** 49P.
Dottori, H. A., 1981. *Astrophys. Space Sci.,* **80,** 267.
Flower, P. J., 1977. *Astr. Astrophys.,* **54,** 31.
Hunter, D. A., Gallagher, J. S. & Rautenkranz, D., 1982. *Astrophys. Suppl. Ser.,* **49,** 53.
Kunth, D. & Sargent, W. L. W., 1983. *Astrophys. J.,* **273,** 81.
Kurucz, R., 1979. *Astrophys. J. Suppl. Ser.,* **40,** 1.
McCall, M. L., Ribsky, P. M. & Shields, G. A., 1985. *Astrophys. J. Suppl. Ser.,* **57,** 1.
Melnick, J., 1985. In: *Star Forming Dwarf Galaxies and Related Objects,* p. 171, eds Kunth, D., Thuan, T. X. & Tran Than Van, J., Ed. Frontiers.
Melnick, J., Moles, M. & Terlevich, R., 1985. *Astr. Astrophys.,* **149,** L24.
Melnick, J., Terlevich, R. & Eggleton, P. P., 1985. *Mon. Not. R. astr. Soc.,* **216,** 255.
Miller, G. E. & Scalo, J. M., 1979. *Astrophys. J. Suppl. Ser.,* **41,** 513.
Rieke, G. H., Lebofsky, M. J., Thompson, R. I., Low, F. J. & Tokunaga, A. T., 1980. *Astrophys. J.,* **238,** 24.
Straizys, V. & Sviderskiene, Z., 1972. *Bull. Vilnius Astr. Obs.,* **35,** 1.
Terlevich, R. J., 1982. *PhD thesis,* University of Cambridge.
Terlevich, R., 1985. In: *Star Forming Dwarf Galaxies and Related Objects,* p. 395, eds Kunth, D., Thuan, T. X. & Tran Than Van, J., Ed. Frontiers.
Tinsley, B. M., 1980. *Fund. Cosmic Phys.,* **5,** 287.
Viallefond, F. & Thuan, T. X., 1983. *Astrophys. J.,* **269,** 444.
Vidal, C. J., Cooper, J. & Smith, E., 1973. *Astrophys. J. Suppl. Ser.,* **25,** 37.
Ward, M. J., Penston, M. V., Blades, J. C. & Turtle, A. J., 1980. *Mon. Not. R. astr. Soc.,* **193,** 563.

Monthly Notices
of the
ROYAL
ASTRONOMICAL SOCIETY

VOL. 231 NO. 1, 1988

Hydrogen absorption line profiles of ionizing star clusters

Angeles I. Díaz

Published for
the Royal Astronomical Society
by
Blackwell Scientific Publications Ltd
Osney Mead
Oxford
OX2 0EL

The microfiches are 105 × 148mm archivally permanent silver halide film produced to internationally accepted standards in the NMA 98-image format

Microfiches produced by Micromedia, Bicester, Oxon

Table 1. Model computed hydrogen line profiles for star clusters formed with a SN IMF ($M_{up}=100M_{\odot}$, $M_{low}=0.08\ M_{\odot}$)

Age = 0.0E+06 yr

λ(Å)	Hdelta	Hgamma	Hbeta	Halpha
0.0	270.4	271.7	291.2	363.3
0.2	307.7	310.7	340.1	412.8
0.4	350.4	356.5	407.2	485.2
0.6	378.2	386.6	449.1	551.3
0.8	398.9	408.2	475.7	592.2
1.0	416.0	425.7	495.0	618.5
1.5	451.4	461.2	529.2	658.2
2.0	482.3	491.6	556.6	682.8
3.0	537.9	545.9	602.8	719.5
4.0	587.4	593.8	642.4	749.1
5.0	631.5	636.6	677.7	774.5
6.0	671.4	675.2	709.2	797.0
8.0	738.2	740.2	762.6	833.9
10.0	790.6	791.6	805.2	863.0
12.0	831.1	831.4	839.5	886.3
14.0	863.2	863.1	866.8	904.7
16.0	887.8	887.4	888.5	920.1
18.0	907.5	907.1	906.4	932.5
20.0	923.0	922.5	920.7	942.4
22.0	935.4	934.8	932.4	950.5
24.0	945.4	944.7	941.9	957.3
28.0	959.8	959.4	956.9	967.5
32.0	970.1	969.8	966.9	975.4
36.0	977.3	977.0	974.6	980.7
40.0	982.2	981.9	979.9	984.9
50.0	990.1	990.0	988.7	991.3
70.0	996.7	996.5	996.2	997.1
W(Å)	13.0	12.0	12.0	9.0

Table 1 (cont.)

Age = 4.0E+06 yr

λ(Å)	Hdelta	Hgamma	Hbeta	Halpha
0.0	222.6	222.0	238.2	304.6
0.2	267.4	269.7	304.1	380.5
0.4	311.2	315.1	376.9	468.6
0.6	339.6	344.8	418.9	539.4
0.8	360.8	366.5	445.8	579.3
1.0	378.2	384.3	465.5	604.4
1.5	413.8	420.1	500.7	643.6
2.0	444.2	450.4	528.5	668.9
3.0	498.0	503.6	574.6	706.3
4.0	545.3	550.2	613.3	736.0
5.0	587.6	591.8	647.7	761.2
6.0	626.3	629.8	678.3	783.1
8.0	693.1	695.6	730.7	819.4
10.0	747.6	749.3	774.0	848.3
12.0	791.6	792.8	810.0	871.9
14.0	827.7	828.5	839.4	891.1
16.0	856.2	856.6	863.5	907.3
18.0	879.8	880.1	883.9	920.7
20.0	898.8	898.9	900.6	931.7
22.0	914.3	914.3	914.4	940.9
24.0	926.9	926.8	925.8	948.7
28.0	945.8	945.8	944.3	960.5
32.0	959.5	959.4	957.1	969.7
36.0	969.0	969.0	966.7	976.1
40.0	975.7	975.6	973.7	981.1
50.0	986.5	986.5	985.1	989.1
70.0	995.4	995.4	994.9	996.3
W(Å)	15.0	14.0	14.0	10.0

Table 1 (cont.)

Age = 6.0E+06 yr

λ(Å)	Hdelta	Hgamma	Hbeta	Halpha
0.0	229.6	229.1	243.9	304.8
0.2	276.6	279.6	313.5	390.7
0.4	322.4	327.2	387.0	479.7
0.6	352.4	358.6	430.7	549.0
0.8	374.7	381.7	458.6	588.9
1.0	393.0	400.3	479.1	614.5
1.5	430.5	438.0	515.9	654.3
2.0	462.2	469.5	544.7	680.1
3.0	517.6	524.1	592.0	718.2
4.0	565.8	571.5	631.2	748.2
5.0	608.2	613.0	665.7	773.2
6.0	646.4	650.3	695.9	794.8
8.0	710.9	713.5	747.2	830.3
10.0	762.3	764.2	788.5	858.1
12.0	803.3	804.4	822.3	880.5
14.0	836.6	837.4	849.6	898.6
16.0	862.9	863.3	871.8	913.7
18.0	884.7	885.0	890.6	926.0
20.0	902.3	902.4	905.9	936.2
22.0	916.7	916.7	918.7	944.7
24.0	928.7	928.6	929.3	951.9
28.0	946.7	946.7	946.4	962.9
32.0	959.8	959.7	958.5	971.3
36.0	969.1	969.1	967.7	977.4
40.0	975.8	975.7	974.4	982.1
50.0	986.5	986.5	985.4	989.5
70.0	995.4	995.4	995.0	996.5
W(Å)	14.0	14.0	13.0	9.0

Table 1 (cont.)

Age = 8.0E+06 yr

λ(Å)	Hdelta	Hgamma	Hbeta	Halpha
0.0	234.8	234.6	250.9	312.4
0.2	283.1	286.8	321.5	403.4
0.4	330.3	336.0	395.4	488.6
0.6	361.3	368.6	440.0	556.9
0.8	384.5	392.4	468.7	597.0
1.0	403.3	411.6	489.8	622.8
1.5	442.0	450.5	527.4	663.0
2.0	474.7	482.9	556.8	689.0
3.0	531.8	539.0	605.0	727.3
4.0	581.0	587.4	644.9	757.4
5.0	624.3	629.6	679.6	782.4
6.0	663.0	667.4	710.1	804.0
8.0	728.0	730.9	761.2	839.0
10.0	779.2	781.4	802.2	866.3
12.0	819.6	821.0	835.3	888.1
14.0	852.0	852.9	862.0	905.6
16.0	877.2	877.8	883.4	920.1
18.0	897.8	898.3	901.3	932.0
20.0	914.2	914.5	915.8	941.6
22.0	927.5	927.6	927.7	949.6
24.0	938.4	938.3	937.6	956.3
28.0	954.3	954.4	953.2	966.5
32.0	965.8	965.8	964.0	974.4
36.0	973.9	973.9	972.2	979.9
40.0	979.5	979.5	978.0	984.1
50.0	988.6	988.6	987.5	990.8
70.0	996.1	996.1	995.7	996.9
W(Å)	13.0	13.0	12.0	9.0

Table 1 (cont.)

Age = 2.0E+07 yr

λ(Å)	Hdelta	Hgamma	Hbeta	Halpha
0.0	229.1	229.5	247.2	312.1
0.2	278.1	282.6	319.0	405.2
0.4	325.0	331.5	393.5	490.2
0.6	355.3	363.4	437.8	558.8
0.8	378.0	386.7	466.0	598.9
1.0	396.5	405.5	486.7	624.3
1.5	434.5	443.7	523.8	663.9
2.0	466.8	475.8	552.9	689.5
3.0	523.6	531.7	600.8	727.5
4.0	573.0	580.2	640.5	757.4
5.0	616.6	622.7	675.4	782.4
6.0	655.9	661.0	706.1	803.9
8.0	722.0	725.5	757.8	838.9
10.0	774.3	776.9	799.3	866.3
12.0	815.5	817.3	832.9	888.2
14.0	848.7	850.0	860.0	905.7
16.0	874.5	875.4	881.7	920.3
18.0	895.6	896.3	899.9	932.2
20.0	912.4	912.8	914.7	941.8
22.0	926.0	926.3	926.7	949.8
24.0	937.1	937.2	936.8	956.5
28.0	953.4	953.5	952.7	966.7
32.0	965.2	965.2	963.6	974.6
36.0	973.4	973.5	971.8	980.0
40.0	979.2	979.2	977.7	984.2
50.0	988.4	988.5	987.4	990.9
70.0	996.1	996.0	995.7	997.0
W(Å)	14.0	13.0	12.0	9.0

Table 1 (cont.)

Age = 4.0E+07 yr

λ(Å)	Hdelta	Hgamma	Hbeta	Halpha
0.0	218.8	219.4	237.9	306.0
0.2	269.4	274.4	312.8	402.7
0.4	316.5	323.5	388.7	488.9
0.6	346.4	354.8	433.0	558.9
0.8	368.6	377.5	460.9	599.0
1.0	386.7	396.0	481.2	624.2
1.5	423.8	433.4	517.6	663.1
2.0	455.4	464.9	546.2	688.3
3.0	511.4	520.1	593.4	725.8
4.0	560.4	568.3	632.9	755.4
5.0	604.1	610.9	667.6	780.2
6.0	643.7	649.5	698.4	801.6
8.0	711.0	715.2	750.5	836.7
10.0	764.8	768.0	792.8	864.2
12.0	807.4	809.7	827.2	886.3
14.0	841.9	843.5	855.0	904.0
16.0	868.7	870.0	877.4	918.8
18.0	890.8	891.7	896.2	930.9
20.0	908.3	908.9	911.5	940.7
22.0	922.5	922.9	923.9	948.8
24.0	934.1	934.3	934.3	955.7
28.0	951.2	951.4	950.8	966.0
32.0	963.5	963.7	962.2	974.0
36.0	972.1	972.3	970.7	979.6
40.0	978.2	978.2	976.9	983.9
50.0	987.9	987.9	986.9	990.7
70.0	995.9	995.8	995.5	996.9
W(Å)	14.0	13.0	13.0	9.0

Table 2. Same as Table 1 but for star clusters formed with a single power-law IMF with x=1.35

Age = 0.0E+06 yr

λ(Å)	Hdelta	Hgamma	Hbeta	Halpha
0.0	395.0	390.7	396.4	446.6
0.2	425.0	422.2	435.2	488.3
0.4	463.0	463.9	491.9	545.5
0.6	490.9	494.4	532.3	601.4
0.8	512.2	517.2	560.1	640.2
1.0	530.0	535.7	580.6	667.4
1.5	566.0	572.2	616.6	710.1
2.0	596.2	602.0	644.0	736.2
3.0	648.0	652.7	687.9	772.3
4.0	692.1	695.0	724.0	799.7
5.0	729.2	731.3	754.9	822.5
6.0	761.8	762.9	781.4	842.1
8.0	814.2	814.2	824.9	873.1
10.0	853.8	853.1	858.3	896.8
12.0	883.4	882.5	884.6	915.3
14.0	906.4	905.4	905.1	929.5
16.0	923.9	922.7	921.1	941.3
18.0	937.6	936.6	934.2	950.7
20.0	948.4	947.3	944.6	958.0
22.0	956.8	955.9	952.9	964.1
24.0	963.5	962.6	959.6	969.2
28.0	973.4	972.8	970.2	976.6
32.0	980.3	979.7	977.2	982.3
36.0	984.9	984.5	982.5	986.1
40.0	988.2	987.9	986.1	989.2
50.0	993.4	993.3	992.3	993.8
70.0	997.8	997.7	997.4	997.9
W(Å)	9.0	9.0	9.0	7.0

Table 2 (cont.)

Age = 4.0E+06 yr

λ(Å)	Hdelta	Hgamma	Hbeta	Halpha
0.0	339.3	338.3	353.3	416.3
0.2	372.9	372.9	395.4	461.4
0.4	415.7	418.9	456.2	522.2
0.6	447.1	453.1	499.4	581.6
0.8	471.3	478.4	528.9	621.7
1.0	491.0	498.8	550.7	649.6
1.5	530.6	538.7	589.4	693.5
2.0	563.7	570.9	618.7	720.6
3.0	619.2	624.9	665.1	758.4
4.0	665.9	669.7	703.3	787.2
5.0	705.4	708.3	735.9	811.1
6.0	739.9	741.8	763.8	831.6
8.0	796.0	796.6	810.1	864.2
10.0	838.8	838.6	845.8	889.2
12.0	871.2	870.7	874.1	908.8
14.0	896.4	895.7	896.2	924.1
16.0	915.6	914.7	913.7	936.6
18.0	930.7	929.8	927.9	946.7
20.0	942.7	941.8	939.3	954.7
22.0	952.0	951.2	948.3	961.2
24.0	959.5	958.6	955.6	966.6
28.0	970.3	969.8	967.3	974.7
32.0	977.9	977.5	975.0	980.9
36.0	983.2	982.9	980.8	984.9
40.0	986.9	986.5	984.7	988.2
50.0	992.6	992.6	991.5	993.3
70.0	997.5	997.4	997.1	997.7
W(Å)	10.0	10.0	10.0	7.0

Table 2 (cont.)

Age = 6.0E+06 yr

λ(Å)	Hdelta	Hgamma	Hbeta	Halpha
0.0	324.8	324.9	341.5	408.0
0.2	359.5	360.6	384.9	454.6
0.4	403.6	407.6	447.2	516.7
0.6	434.9	441.7	490.9	577.2
0.8	458.6	466.7	520.3	617.7
1.0	478.0	486.6	541.7	645.6
1.5	517.2	525.8	579.5	688.9
2.0	550.1	557.9	608.5	715.5
3.0	606.3	612.4	655.4	753.0
4.0	653.7	658.3	693.9	782.0
5.0	694.6	697.8	727.3	806.1
6.0	730.3	732.3	755.9	826.9
8.0	788.3	788.9	803.6	860.2
10.0	832.5	832.4	840.4	885.8
12.0	866.0	865.5	869.6	905.9
14.0	892.2	891.5	892.5	921.7
16.0	912.1	911.2	910.4	934.6
18.0	927.8	927.0	925.1	945.0
20.0	940.2	939.4	936.8	953.3
22.0	949.9	949.2	946.3	959.9
24.0	957.7	956.9	953.9	965.4
28.0	969.0	968.5	966.0	973.8
32.0	977.0	976.6	973.9	980.1
36.0	982.5	982.2	980.0	984.5
40.0	986.3	985.9	984.2	987.8
50.0	992.3	992.2	991.2	993.1
70.0	997.4	997.3	997.0	997.6
W(Å)	10.0	10.0	10.0	7.0

Table 2 (cont.)

Age = 8.0E+06 yr

λ(Å)	Hdelta	Hgamma	Hbeta	Halpha
0.0	301.4	302.6	322.1	393.1
0.2	337.5	340.0	367.3	441.7
0.4	382.9	388.3	432.0	506.3
0.6	414.5	422.7	476.3	568.4
0.8	438.3	447.5	505.7	609.7
1.0	457.6	467.4	527.3	637.9
1.5	497.1	506.7	564.9	681.1
2.0	530.9	539.5	594.2	707.5
3.0	589.5	595.9	642.4	745.4
4.0	639.2	644.0	682.4	775.1
5.0	681.9	685.2	717.1	799.9
6.0	719.1	721.3	747.0	821.4
8.0	779.5	780.1	796.2	855.7
10.0	825.3	825.2	834.4	882.2
12.0	860.1	859.6	864.4	902.7
14.0	887.3	886.6	888.1	919.0
16.0	908.0	907.1	906.8	932.3
18.0	924.4	923.6	922.0	943.0
20.0	937.3	936.5	934.1	951.5
22.0	947.4	946.7	943.8	958.4
24.0	955.7	954.9	952.0	964.2
28.0	967.5	967.0	964.4	972.9
32.0	975.8	975.4	972.8	979.5
36.0	981.6	981.3	979.1	983.9
40.0	985.6	985.3	983.5	987.5
50.0	992.0	991.9	990.7	992.7
70.0	997.1	997.1	996.8	997.6
W(Å)	11.0	11.0	10.0	8.0

Table 2 (cont.)

Age = 2.0E+07 yr

λ(Å)	Hdelta	Hgamma	Hbeta	Halpha
0.0	276.6	279.1	300.7	376.2
0.2	314.1	318.1	348.9	428.5
0.4	358.1	365.4	415.2	496.4
0.6	387.3	397.0	458.0	560.5
0.8	409.1	419.8	485.4	601.4
1.0	427.1	438.1	505.4	628.2
1.5	464.2	475.1	540.8	668.6
2.0	496.6	506.7	569.1	693.7
3.0	554.6	562.8	616.5	730.6
4.0	605.5	611.9	657.0	760.3
5.0	650.2	655.1	692.7	785.6
6.0	690.0	693.5	724.2	807.9
8.0	755.4	757.0	776.8	844.0
10.0	805.7	806.4	818.0	872.1
12.0	844.2	844.2	850.8	894.4
14.0	874.3	874.1	876.7	911.8
16.0	897.3	896.8	897.2	926.2
18.0	915.6	915.2	913.9	937.9
20.0	930.0	929.4	927.2	947.1
22.0	941.3	940.8	938.1	954.7
24.0	950.5	949.9	946.9	961.0
28.0	963.6	963.3	960.8	970.3
32.0	973.0	972.7	970.0	977.6
36.0	979.5	979.3	977.0	982.4
40.0	984.0	983.7	981.9	986.3
50.0	991.0	991.0	989.8	992.1
70.0	996.9	996.8	996.5	997.4
W(Å)	12.0	12.0	11.0	8.0

Table 2 (cont.)

Age = 4.0E+07 yr

λ(Å)	Hdelta	Hgamma	Hbeta	Halpha
0.0	248.6	250.4	272.0	349.0
0.2	288.9	292.9	325.5	406.9
0.4	333.3	340.5	396.0	480.8
0.6	361.1	370.6	438.6	549.5
0.8	381.8	391.9	465.1	590.9
1.0	398.7	409.1	483.9	616.9
1.5	433.9	444.4	517.9	655.8
2.0	464.8	474.9	545.2	680.0
3.0	521.0	529.6	591.5	716.2
4.0	571.4	578.5	631.6	745.9
5.0	616.6	622.4	667.5	771.3
6.0	657.9	662.3	699.7	793.8
8.0	727.1	729.7	754.5	831.1
10.0	781.7	783.4	798.6	860.7
12.0	824.1	824.8	834.0	884.3
14.0	857.6	857.9	862.4	903.1
16.0	883.3	883.4	884.9	918.7
18.0	904.0	904.0	903.4	931.4
20.0	920.2	919.9	918.3	941.6
22.0	933.1	932.7	930.3	949.8
24.0	943.6	942.9	940.3	956.7
28.0	958.5	958.3	955.7	967.1
32.0	969.2	969.0	966.1	975.0
36.0	976.6	976.4	974.0	980.6
40.0	981.7	981.4	979.5	984.7
50.0	989.8	989.8	988.5	991.2
70.0	996.6	996.4	996.1	997.1
W(Å)	13.0	13.0	12.0	9.0

Table 3. Same as Table 1 but for star clusters formed with a single power-law IMF with x=2.05

Age = 0.0E+06 yr

λ(Å)	Hdelta	Hgamma	Hbeta	Halpha
0.0	282.8	280.6	292.7	351.8
0.2	326.8	329.0	360.4	452.7
0.4	369.7	374.6	428.0	526.2
0.6	398.5	405.2	469.9	588.5
0.8	420.1	427.7	497.2	626.3
1.0	437.9	446.0	517.1	650.9
1.5	474.4	482.6	552.7	689.0
2.0	505.3	513.3	580.4	713.2
3.0	559.7	566.6	625.9	748.4
4.0	607.0	612.6	663.9	776.1
5.0	648.4	653.0	697.2	799.3
6.0	685.6	689.2	726.4	819.4
8.0	747.8	749.9	775.6	852.0
10.0	796.7	797.9	814.9	877.6
12.0	834.8	835.4	846.6	898.0
14.0	865.2	865.4	871.9	914.2
16.0	888.8	888.7	892.2	927.6
18.0	907.8	907.7	909.1	938.6
20.0	922.9	922.6	922.7	947.4
22.0	935.0	934.7	933.8	954.7
24.0	944.8	944.4	942.9	960.9
28.0	959.3	959.1	957.4	970.1
32.0	969.6	969.4	967.3	977.2
36.0	976.8	976.6	974.7	982.1
40.0	981.9	981.7	980.0	985.9
50.0	989.9	989.9	988.7	991.9
70.0	996.6	996.5	996.2	997.3
W(Å)	12.0	12.0	11.0	8.0

Table 3 (cont.)

Age =4.0E+06 yr

λ(Å)	Hdelta	Hgamma	Hbeta	Halpha
0.0	267.1	266.3	281.4	344.8
0.2	312.4	315.8	350.4	447.3
0.4	356.7	362.5	419.1	521.7
0.6	386.4	394.1	461.8	584.7
0.8	408.8	417.2	489.5	622.8
1.0	427.2	436.0	509.8	647.5
1.5	464.6	473.5	546.1	685.9
2.0	496.3	504.8	574.3	710.3
3.0	551.5	558.9	620.3	745.9
4.0	599.4	605.5	658.7	773.8
5.0	641.4	646.4	692.3	797.1
6.0	679.0	683.0	721.9	817.3
8.0	742.2	744.6	771.7	850.2
10.0	791.9	793.5	811.5	876.0
12.0	830.8	831.7	843.7	896.6
14.0	861.9	862.4	869.4	913.0
16.0	886.0	886.1	890.1	926.6
18.0	905.4	905.5	907.3	937.7
20.0	921.0	920.8	921.2	946.7
22.0	933.3	933.2	932.4	954.1
24.0	943.4	943.1	941.8	960.3
28.0	958.2	958.1	956.6	969.6
32.0	968.8	968.7	966.6	976.9
36.0	976.2	976.1	974.2	981.8
40.0	981.4	981.2	979.6	985.7
50.0	989.6	989.6	988.5	991.7
70.0	996.5	996.4	996.1	997.2
W(Å)	13.0	12.0	12.0	8.0

Table 3 (cont.)

Age = 6.0E+06 yr

λ(Å)	Hdelta	Hgamma	Hbeta	Halpha
0.0	260.7	260.5	276.6	341.9
0.2	306.6	310.7	346.4	445.4
0.4	351.5	357.8	415.8	520.2
0.6	381.3	389.4	458.7	583.6
0.8	403.5	412.5	486.4	621.9
1.0	421.8	431.0	506.5	646.6
1.5	459.0	468.3	542.4	684.7
2.0	490.6	499.5	570.5	708.9
3.0	546.2	553.8	616.7	744.4
4.0	594.3	600.8	655.3	772.3
5.0	636.9	642.1	689.2	795.7
6.0	675.0	679.1	718.9	816.0
8.0	738.8	741.4	769.2	849.1
10.0	789.1	790.8	809.4	875.0
12.0	828.5	829.5	841.9	895.7
14.0	860.0	860.5	867.9	912.3
16.0	884.3	884.5	888.8	926.0
18.0	904.1	904.2	906.2	937.2
20.0	919.8	919.7	920.1	946.2
22.0	932.3	932.2	931.6	953.6
24.0	942.6	942.3	941.0	959.9
28.0	957.6	957.5	956.0	969.4
32.0	968.3	968.2	966.2	976.6
36.0	975.8	975.8	973.9	981.7
40.0	981.1	980.9	979.4	985.5
50.0	989.5	989.4	988.3	991.7
70.0	996.4	996.3	996.0	997.2
W(Å)	13.0	12.0	12.0	8.0

Table 3 (cont.)

Age = 8.0E+06 yr

λ(Å)	Hdelta	Hgamma	Hbeta	Halpha
0.0	252.7	253.0	270.3	337.6
0.2	299.4	304.0	341.1	442.1
0.4	345.0	351.8	411.3	517.7
0.6	375.1	383.7	454.6	581.6
0.8	397.6	406.9	482.5	620.1
1.0	415.9	425.5	502.8	644.9
1.5	453.4	463.1	538.8	683.2
2.0	485.5	494.6	567.1	707.4
3.0	542.0	549.7	613.8	743.0
4.0	590.8	597.3	652.8	771.2
5.0	633.8	639.0	687.0	794.7
6.0	672.2	676.4	717.1	815.2
8.0	736.5	739.1	767.6	848.4
10.0	787.1	788.8	808.0	874.5
12.0	826.7	827.8	840.6	895.2
14.0	858.4	859.0	866.8	911.8
16.0	883.0	883.2	887.8	925.6
18.0	903.0	903.1	905.3	936.8
20.0	918.8	918.8	919.4	945.9
22.0	931.5	931.4	930.9	953.3
24.0	941.9	941.6	940.5	959.6
28.0	957.0	957.0	955.5	969.1
32.0	967.9	967.8	965.8	976.5
36.0	975.5	975.5	973.6	981.5
40.0	980.8	980.7	979.2	985.5
50.0	989.4	989.3	988.2	991.6
70.0	996.3	996.3	996.0	997.2
W(Å)	13.0	12.0	12.0	8.0

Table 3 (cont.)

Age = 2.0E+07 yr

λ(Å)	Hdelta	Hgamma	Hbeta	Halpha
0.0	242.2	243.2	261.7	331.4
0.2	289.7	295.3	334.2	438.5
0.4	334.9	342.6	405.2	515.2
0.6	364.0	373.5	448.0	579.8
0.8	385.7	395.8	475.1	618.0
1.0	403.6	413.9	494.8	642.4
1.5	440.2	450.6	530.0	679.7
2.0	471.7	481.7	558.0	703.5
3.0	527.9	536.6	604.4	738.7
4.0	577.2	584.6	643.5	766.8
5.0	620.9	627.0	678.1	790.5
6.0	660.3	665.3	708.6	811.1
8.0	726.5	729.8	760.3	844.9
10.0	778.9	781.1	801.9	871.4
12.0	820.0	821.4	835.4	892.6
14.0	852.9	853.8	862.4	909.6
16.0	878.4	878.9	884.1	923.7
18.0	899.1	899.5	902.2	935.2
20.0	915.6	915.7	916.7	944.5
22.0	928.8	928.9	928.6	952.2
24.0	939.6	939.5	938.5	958.6
28.0	955.3	955.3	954.1	968.3
32.0	966.6	966.6	964.7	975.9
36.0	974.6	974.6	972.7	981.0
40.0	980.1	980.0	978.5	985.1
50.0	988.9	989.0	987.8	991.4
70.0	996.2	996.1	995.8	997.1
W(Å)	13.0	13.0	12.0	8.0

Table 3 (cont.)

Age = 4.0E+07 yr

λ(Å)	Hdelta	Hgamma	Hbeta	Halpha
0.0	226.9	227.8	247.0	319.1
0.2	276.5	282.4	323.2	430.8
0.4	322.0	330.1	396.4	510.2
0.6	350.7	360.3	439.2	576.5
0.8	371.9	382.0	465.9	614.9
1.0	389.3	399.7	485.2	638.9
1.5	425.2	435.7	519.9	675.6
2.0	456.0	466.3	547.5	699.0
3.0	511.4	520.6	593.4	733.9
4.0	560.5	568.6	632.4	762.0
5.0	604.4	611.3	667.0	785.6
6.0	644.4	650.2	697.8	806.3
8.0	712.4	716.4	750.4	840.3
10.0	766.8	769.8	793.1	867.3
12.0	809.7	811.7	827.7	889.0
14.0	844.2	845.6	855.8	906.4
16.0	871.0	872.1	878.4	920.9
18.0	893.0	893.7	897.2	932.8
20.0	910.4	910.8	912.5	942.4
22.0	924.3	924.6	924.9	950.3
24.0	935.8	935.8	935.3	957.0
28.0	952.5	952.7	951.6	967.1
32.0	964.6	964.7	962.8	974.9
36.0	973.0	973.0	971.3	980.3
40.0	978.9	978.8	977.3	984.5
50.0	988.3	988.3	987.2	991.0
70.0	996.0	995.9	995.6	997.0
W(Å)	14.0	13.0	13.0	8.0

Table 4. Same as Table 1 but for star clusters formed with a single power-law IMF with x=2.35

Age = 0.0E+06 yr

λ(Å)	Hdelta	Hgamma	Hbeta	Halpha
0.0	253.8	252.5	266.4	329.7
0.2	305.5	310.6	350.9	467.9
0.4	350.0	357.3	421.3	543.6
0.6	379.3	388.1	463.6	604.9
0.8	401.2	410.7	490.8	641.0
1.0	419.2	429.0	510.6	664.1
1.5	456.0	466.0	546.2	700.0
2.0	487.1	496.8	573.9	723.1
3.0	541.7	550.4	619.4	756.9
4.0	589.2	596.7	657.2	783.5
5.0	631.0	637.4	690.3	805.7
6.0	668.7	674.1	719.4	824.8
8.0	732.3	736.0	768.6	856.0
10.0	782.7	785.4	808.1	880.5
12.0	822.4	824.2	840.2	900.0
14.0	854.3	855.6	866.0	915.6
16.0	879.2	880.0	886.9	928.7
18.0	899.5	900.1	904.3	939.3
20.0	915.7	916.1	918.4	947.9
22.0	928.7	929.0	929.9	955.1
24.0	939.4	939.5	939.4	961.1
28.0	955.1	955.3	954.7	970.2
32.0	966.5	966.5	965.1	977.2
36.0	974.4	974.4	973.0	982.1
40.0	979.9	979.9	978.6	985.9
50.0	988.8	988.9	987.9	991.8
70.0	996.2	996.2	995.9	997.3
W(Å)	13.0	13.0	12.0	8.0

Table 4 (cont.)

Age = 4.0E+06 yr

λ(Å)	Hdelta	Hgamma	Hbeta	Halpha
0.0	245.5	245.0	260.6	326.5
0.2	297.9	303.9	346.0	465.7
0.4	343.2	351.1	417.0	541.8
0.6	373.1	382.4	459.6	603.4
0.8	395.4	405.4	487.1	639.6
1.0	413.7	424.0	507.1	662.7
1.5	450.9	461.3	543.0	698.7
2.0	482.5	492.5	571.0	721.9
3.0	537.5	546.5	616.7	755.9
4.0	585.3	593.1	654.7	782.6
5.0	627.4	634.0	688.0	804.8
6.0	665.3	670.9	717.2	824.0
8.0	729.3	733.3	766.6	855.3
10.0	780.1	783.0	806.4	879.8
12.0	820.2	822.3	838.8	899.4
14.0	852.5	854.0	864.8	915.2
16.0	877.7	878.6	885.8	928.2
18.0	898.2	898.9	903.3	938.9
20.0	914.6	915.1	917.6	947.6
22.0	927.8	928.2	929.2	954.8
24.0	938.6	938.8	938.9	960.8
28.0	954.6	954.7	954.2	970.0
32.0	966.0	966.1	964.8	977.1
36.0	974.0	974.1	972.7	981.9
40.0	979.7	979.7	978.4	985.8
50.0	988.7	988.7	987.8	991.8
70.0	996.1	996.1	995.8	997.3
W(Å)	13.0	13.0	12.0	8.0

Table 4 (cont.)

Age = 6.0E+06 yr

λ(Å)	Hdelta	Hgamma	Hbeta	Halpha
0.0	241.3	241.3	257.6	324.8
0.2	294.2	300.6	343.6	464.8
0.4	339.9	348.2	415.0	541.1
0.6	369.8	379.5	457.8	602.9
0.8	392.0	402.4	485.2	639.2
1.0	410.2	420.8	505.2	662.3
1.5	447.4	458.1	540.8	698.2
2.0	478.9	489.2	568.8	721.2
3.0	534.1	543.3	614.6	755.2
4.0	582.1	590.2	652.7	781.9
5.0	624.5	631.4	686.1	804.1
6.0	662.7	668.5	715.5	823.4
8.0	727.2	731.2	765.2	854.7
10.0	778.3	781.4	805.2	879.3
12.0	818.7	820.8	837.7	899.0
14.0	851.3	852.8	863.9	914.8
16.0	876.6	877.6	885.0	927.9
18.0	897.3	898.1	902.7	938.7
20.0	913.8	914.3	917.0	947.4
22.0	927.1	927.5	928.7	954.6
24.0	938.0	938.2	938.4	960.6
28.0	954.1	954.3	953.9	969.8
32.0	965.7	965.8	964.5	976.9
36.0	973.8	973.9	972.5	981.9
40.0	979.5	979.5	978.3	985.7
50.0	988.6	988.6	987.7	991.7
70.0	996.1	996.1	995.8	997.2
W(Å)	13.0	13.0	12.0	8.0

Table 4 (cont.)

Age = 8.0+06 yr

λ(Å)	Hdelta	Hgamma	Hbeta	Halpha
0.0	236.8	237.0	254.1	322.6
0.2	290.1	296.9	340.8	463.2
0.4	336.4	344.9	412.7	540.0
0.6	366.5	376.5	455.7	602.0
0.8	388.9	399.5	483.3	638.4
1.0	407.2	418.0	503.4	661.6
1.5	444.6	455.5	539.2	697.6
2.0	476.4	486.9	567.3	720.7
3.0	532.3	541.4	613.4	754.8
4.0	580.6	588.7	651.7	781.5
5.0	623.2	630.0	685.3	803.9
6.0	661.5	667.3	714.8	823.1
8.0	726.1	730.2	764.6	854.6
10.0	777.4	780.4	804.7	879.2
12.0	817.9	820.0	837.1	898.8
14.0	850.5	852.0	863.4	914.6
16.0	875.9	877.0	884.6	927.8
18.0	896.7	897.6	902.3	938.5
20.0	913.3	913.9	916.6	947.2
22.0	926.7	927.1	928.3	954.4
24.0	937.7	937.9	938.1	960.5
28.0	953.8	954.1	953.7	969.8
32.0	965.4	965.6	964.3	976.9
36.0	973.6	973.7	972.4	981.8
40.0	979.3	979.4	978.2	985.7
50.0	988.5	988.6	987.6	991.7
70.0	996.1	996.0	995.8	997.2
W(Å)	13.0	13.0	12.0	8.0

Table 4 (cont.)

Age = 2.0E+07 yr

λ(Å)	Hdelta	Hgamma	Hbeta	Halpha
0.0	230.0	230.8	248.8	319.1
0.2	284.0	291.5	336.8	461.6
0.4	330.0	339.3	409.1	539.0
0.6	359.5	370.2	451.8	601.3
0.8	381.5	392.7	478.9	637.6
1.0	399.5	410.9	498.7	660.5
1.5	436.3	447.8	534.0	695.9
2.0	467.8	478.9	561.9	718.7
3.0	523.4	533.4	607.8	752.6
4.0	572.0	580.8	646.2	779.3
5.0	615.1	622.6	680.0	801.7
6.0	654.0	660.4	709.8	821.1
8.0	719.8	724.4	760.3	852.7
10.0	772.1	775.6	801.0	877.6
12.0	813.6	816.0	834.1	897.5
14.0	846.9	848.7	860.8	913.5
16.0	872.9	874.2	882.3	926.8
18.0	894.2	895.3	900.4	937.7
20.0	911.2	911.9	915.0	946.5
22.0	924.9	925.5	927.0	953.8
24.0	936.2	936.5	936.9	960.0
28.0	952.7	953.0	952.8	969.3
32.0	964.6	964.8	963.6	976.6
36.0	973.0	973.1	971.9	981.5
40.0	978.9	978.9	977.8	985.5
50.0	988.2	988.3	987.4	991.6
70.0	996.0	995.9	995.7	997.2
W(Å)	14.0	13.0	12.0	8.0

Table 4 (cont.)

Age = 4.0E+07 yr

λ(Å)	Hdelta	Hgamma	Hbeta	Halpha
0.0	218.8	219.6	238.4	311.1
0.2	274.6	282.5	329.5	457.5
0.4	320.9	330.6	403.4	536.5
0.6	350.2	361.1	446.2	599.9
0.8	371.9	383.2	473.1	636.2
1.0	389.6	401.1	492.5	658.9
1.5	425.9	437.6	527.5	693.8
2.0	457.0	468.4	555.2	716.4
3.0	512.1	522.5	600.8	750.1
4.0	560.5	569.9	639.0	776.7
5.0	603.7	611.9	672.8	799.1
6.0	643.1	650.2	702.8	818.4
8.0	710.0	715.3	753.8	850.2
10.0	763.7	767.8	795.3	875.3
12.0	806.3	809.3	829.0	895.4
14.0	840.8	843.0	856.4	911.7
16.0	867.7	869.5	878.5	925.2
18.0	889.9	891.2	897.1	936.3
20.0	907.5	908.5	912.2	945.3
22.0	921.7	922.5	924.5	952.8
24.0	933.4	933.9	934.8	959.1
28.0	950.7	951.1	951.1	968.6
32.0	963.1	963.5	962.4	976.0
36.0	971.8	972.1	970.9	981.1
40.0	978.0	978.0	977.0	985.1
50.0	987.8	987.9	986.9	991.4
70.0	995.8	995.8	995.6	997.1
W(Å)	14.0	13.0	12.0	8.0

Table 5. Same as Table 1 but for star clusters formed with a single power-law IMF with x=2.65

Age = 0.0E+06 yr

λ(Å)	Hdelta	Hgamma	Hbeta	Halpha
0.0	233.4	232.9	248.4	317.0
0.2	294.3	303.2	353.8	500.7
0.4	340.3	350.9	425.9	575.4
0.6	370.3	382.0	468.2	633.4
0.8	392.6	404.8	495.3	667.0
1.0	410.8	423.3	515.1	688.2
1.5	448.0	460.5	550.6	721.4
2.0	479.3	491.5	578.2	743.0
3.0	534.0	545.1	623.2	774.8
4.0	581.2	591.3	660.3	799.6
5.0	622.9	631.7	692.7	820.1
6.0	660.4	668.1	721.2	837.8
8.0	724.1	729.8	769.2	866.5
10.0	774.8	779.3	807.9	888.9
12.0	815.1	818.5	839.5	906.9
14.0	847.7	850.3	865.0	921.3
16.0	873.2	875.1	885.6	933.3
18.0	894.2	895.7	903.0	943.1
20.0	911.0	912.2	917.1	951.1
22.0	924.5	925.5	928.6	957.7
24.0	935.7	936.4	938.2	963.4
28.0	952.3	952.9	953.6	971.9
32.0	964.3	964.7	964.3	978.5
36.0	972.7	973.0	972.3	983.0
40.0	978.6	978.8	978.1	986.6
50.0	988.1	988.2	987.6	992.2
70.0	995.9	995.9	995.8	997.4
W(Å)	14.0	13.0	12.0	7.0

Table 5 (cont.)

Age = 4.0E+06 yr

λ(Å)	Hdelta	Hgamma	Hbeta	Halpha
0.0	229.1	229.2	245.6	315.6
0.2	290.5	299.9	351.5	499.9
0.4	336.9	347.8	423.8	574.7
0.6	367.2	379.2	466.3	632.9
0.8	389.7	402.2	493.5	666.5
1.0	408.1	420.8	513.5	687.7
1.5	445.6	458.3	549.1	720.9
2.0	477.1	489.5	576.9	742.6
3.0	531.9	543.2	622.0	774.4
4.0	579.3	589.5	659.2	799.2
5.0	621.1	630.0	691.7	819.8
6.0	658.7	666.6	720.2	837.5
8.0	722.6	728.5	768.3	866.2
10.0	773.5	778.1	807.2	888.7
12.0	814.0	817.5	838.8	906.7
14.0	846.7	849.4	864.4	921.1
16.0	872.4	874.4	885.1	933.1
18.0	893.5	895.1	902.5	943.0
20.0	910.4	911.6	916.7	951.0
22.0	924.1	925.1	928.3	957.6
24.0	935.3	936.1	938.0	963.3
28.0	952.0	952.6	953.4	971.8
32.0	964.0	964.5	964.1	978.4
36.0	972.5	972.8	972.2	983.0
40.0	978.5	978.7	978.0	986.6
50.0	988.0	988.2	987.5	992.2
70.0	995.9	995.9	995.7	997.4
W(Å)	14.0	13.0	12.0	7.0

Table 5 (cont.)

Age = 6.0E+06 yr

λ(Å)	Hdelta	Hgamma	Hbeta	Halpha
0.0	226.4	226.8	243.7	314.7
0.2	288.2	297.9	350.2	499.5
0.4	334.9	346.1	422.7	574.5
0.6	365.1	377.4	465.3	632.7
0.8	387.6	400.4	492.5	666.4
1.0	406.0	418.9	512.4	687.6
1.5	443.4	456.3	547.9	720.7
2.0	474.9	487.5	575.7	742.3
3.0	529.9	541.3	620.8	774.1
4.0	577.3	587.8	658.1	798.9
5.0	619.3	628.4	690.6	819.5
6.0	657.2	665.1	719.2	837.2
8.0	721.3	727.3	767.5	866.0
10.0	772.4	777.1	806.5	888.4
12.0	813.0	816.6	838.2	906.5
14.0	845.9	848.7	863.9	920.9
16.0	871.7	873.8	884.7	933.0
18.0	892.9	894.6	902.1	942.8
20.0	909.9	911.2	916.3	950.9
22.0	923.6	924.7	928.0	957.5
24.0	934.9	935.7	937.7	963.2
28.0	951.7	952.3	953.2	971.7
32.0	963.8	964.3	963.9	978.3
36.0	972.3	972.7	972.0	982.9
40.0	978.3	978.5	977.9	986.5
50.0	988.0	988.1	987.4	992.2
70.0	995.9	995.9	995.7	997.4
W(Å)	14.0	13.0	12.0	7.0

Table 5 (cont.)

Age = 8.0E+06 yr

λ(Å)	Hdelta	Hgamma	Hbeta	Halpha
0.0	224.0	224.5	241.9	313.7
0.2	286.0	296.0	348.7	498.9
0.4	333.1	344.4	421.6	574.1
0.6	363.5	376.0	464.4	632.4
0.8	386.1	399.0	491.7	666.1
1.0	404.6	417.6	511.6	687.4
1.5	442.2	455.2	547.3	720.6
2.0	473.9	486.5	575.1	742.2
3.0	529.2	540.6	620.4	774.0
4.0	576.9	587.3	657.8	798.9
5.0	619.0	628.0	690.4	819.5
6.0	656.8	664.7	719.1	837.2
8.0	720.9	726.9	767.3	866.0
10.0	772.0	776.7	806.3	888.4
12.0	812.7	816.3	838.0	906.4
14.0	845.6	848.4	863.7	920.9
16.0	871.4	873.5	884.5	932.9
18.0	892.6	894.4	902.0	942.8
20.0	909.6	911.0	916.2	950.8
22.0	923.4	924.5	927.8	957.5
24.0	934.7	935.5	937.6	963.2
28.0	951.6	952.2	953.1	971.7
32.0	963.7	964.2	963.9	978.3
36.0	972.2	972.6	972.0	982.9
40.0	978.3	978.5	977.8	986.5
50.0	987.9	988.1	987.4	992.2
70.0	995.9	995.9	995.7	997.4
W(Å)	14.0	13.0	12.0	7.0

Table 5 (cont.)

Age = 2.0E+07 yr

λ(Å)	Hdelta	Hgamma	Hbeta	Halpha
0.0	219.7	220.7	238.7	311.8
0.2	282.3	292.7	346.6	498.3
0.4	329.2	341.1	419.7	573.8
0.6	359.3	372.2	462.2	632.2
0.8	381.7	395.0	489.3	665.8
1.0	399.9	413.4	509.1	686.9
1.5	437.2	450.7	544.4	719.9
2.0	468.7	481.8	572.1	741.3
3.0	523.9	535.9	617.3	773.0
4.0	571.7	582.6	654.7	797.9
5.0	614.1	623.6	687.5	818.5
6.0	652.3	660.7	716.3	836.2
8.0	717.1	723.5	764.9	865.1
10.0	768.9	773.9	804.3	887.7
12.0	810.1	813.9	836.3	905.8
14.0	843.4	846.4	862.2	920.3
16.0	869.6	871.9	883.2	932.5
18.0	891.1	893.0	900.9	942.4
20.0	908.3	909.8	915.3	950.5
22.0	922.3	923.5	927.1	957.2
24.0	933.8	934.7	936.9	962.9
28.0	950.9	951.6	952.6	971.5
32.0	963.2	963.7	963.5	978.2
36.0	971.8	972.2	971.7	982.8
40.0	978.0	978.2	977.6	986.4
50.0	987.7	987.9	987.3	992.1
70.0	995.8	995.8	995.7	997.4
W(Å)	14.0	13.0	12.0	7.0

Table 5 (cont.)

Age = 4.0E+07 yr

λ(Å)	Hdelta	Hgamma	Hbeta	Halpha
0.0	211.8	212.9	231.7	307.0
0.2	275.9	286.8	342.1	496.4
0.4	323.1	335.3	416.3	572.9
0.6	353.0	366.3	458.8	631.9
0.8	375.2	388.8	485.7	665.5
1.0	393.3	407.0	505.3	686.4
1.5	430.3	444.0	540.5	719.0
2.0	461.5	475.0	568.1	740.3
3.0	516.4	528.8	613.1	771.9
4.0	564.1	575.6	650.4	796.7
5.0	606.5	616.6	683.1	817.3
6.0	645.0	653.9	712.0	834.9
8.0	710.6	717.5	760.9	863.9
10.0	763.2	768.7	800.7	886.5
12.0	805.2	809.4	833.2	904.8
14.0	839.3	842.6	859.5	919.4
16.0	866.0	868.7	880.9	931.6
18.0	888.1	890.3	898.8	941.7
20.0	905.8	907.5	913.5	949.9
22.0	920.1	921.5	925.5	956.7
24.0	931.9	933.0	935.5	962.4
28.0	949.5	950.3	951.5	971.1
32.0	962.2	962.8	962.7	977.9
36.0	971.0	971.5	971.1	982.6
40.0	977.3	977.6	977.1	986.2
50.0	987.4	987.6	987.0	992.0
70.0	995.7	995.7	995.6	997.3
W(Å)	14.0	13.0	12.0	7.0